

# Comprehensive analysis of circRNAs from steatotic livers after ischemia and reperfusion injury by next generation RNA sequencing

## Xiaoye Qu

<sup>1</sup>Department of Liver Surgery, Renji Hospital, School of Medicine, Shanghai Jiao Tong University, Shanghai, China <sup>2</sup>Institute of Clinical Immunology, Department of Liver Diseases, Central Laboratory, ShuGuang Hospital, Shanghai, China

## Chao Zheng

Institute of Clinical Immunology, Department of Liver Diseases, Central Laboratory, ShuGuang Hospital Affiliated to Shanghai University of Chinese Traditional Medicine, Shanghai, China

## Bingrui Wang

<sup>1</sup>Department of Liver Surgery, Renji Hospital, School of Medicine, Shanghai Jiao Tong University, Shanghai, China <sup>2</sup>Institute of Clinical Immunology, Department of Liver Diseases, Central Laboratory, ShuGuang Hospital, Shanghai, China

## Fang Wang

Institute of Clinical Immunology, Department of Liver Diseases, Central Laboratory, ShuGuang Hospital Affiliated to Shanghai University of Chinese Traditional Medicine, Shanghai, China

## Xuehua Sun

Institute of Clinical Immunology, Department of Liver Diseases, Central Laboratory, ShuGuang Hospital Affiliated to Shanghai University of Chinese Traditional Medicine, Shanghai, China

## Yueqiu Gao

Institute of Clinical Immunology, Department of Liver Diseases, Central Laboratory, ShuGuang Hospital Affiliated to Shanghai University of Chinese Traditional Medicine, Shanghai, China

## Qiang Xia

Department of Liver Surgery, Renji Hospital, School of Medicine, Shanghai Jiao Tong University, Shanghai, China

## Xiaoni Kong (✉ [xiaoni-kong@126.com](mailto:xiaoni-kong@126.com))

Institute of Clinical Immunology, Department of Liver Diseases, Central Laboratory, ShuGuang Hospital Affiliated to Shanghai University of Chinese Traditional Medicine, Shanghai, China

---

## Research

**Keywords:** Circular RNA, Hepatic steatosis, liver ischemia/reperfusion injury, Bioinformatics analysis, Circularity

**Posted Date:** March 18th, 2020

**DOI:** <https://doi.org/10.21203/rs.3.rs-17696/v1>

**License:**  This work is licensed under a Creative Commons Attribution 4.0 International License.

[Read Full License](#)

---

# Abstract

**Background** Global organ shortage has enabled the permission of fatty livers for transplantation purpose, taking the risk of graft dysfunction related to the rapider ischemia/reperfusion injury (IRI) progress. Increasing evidence supports the role of circular RNAs as essential regulators of this progress. However, data about circular RNAs in ischemia and reperfusion injured steatotic livers are practically nonexistent.

**Methods** In the present study, high-fat diet (HFD)-fed mice model was used to generate hepatic steatosis mice. RNA-sequencing was performed on IRI model or sham liver tissues both in HFD-fed mice to screen the significant differentially expressed circular RNAs. GO and KEGG analysis were applied to figure out the potential function of these screened circular RNAs.

**Results** From this, we successfully found the expression of some circular RNAs were significantly altered in IRI livers after HFD-fed mouse models. To further validate sequencing data, one up-regulated circRNA and four down-regulated circular RNAs were examined in steatotic mice livers after IRI. The RNase R digestion experiment exhibited these circRNAs possessed high stability compared with linear RNAs and sequence alignment of their junction positions provided identical sequences by sanger sequencing following gel electrophoresis, demonstrating the circularity of these circular RNAs. The expression of four stable circRNAs undigested by RNase R were further validated by quantitative PCR.

**Conclusion** In summary, this study reveals that circular RNAs emerge as novel and potentially efficient targets which involve in more severe damage of steatotic livers to IRI.

## Background

Liver transplantation has become an effective treatment strategy for chronic end-stage liver disease [1, 2]. Ischemia and reperfusion injury (IRI) remains a primary clinical issue during the development of transplantation surgery [3]. Numerous adverse pathophysiological events, including inflammatory responses, oxidative stress and mitochondrial dysfunction occur following the hepatic IRI [4]. As the rapidly increase of the obese adult proportion in recent years and the decrease of organs available for graft, fatty livers have been used to remedy this situation, which may compromise the overall success of liver transplantation [5, 6]. Moderate to severe hepatic steatosis leads to higher possibility of organ dysfunction or non-function [7]. A steatotic liver, compared with a lean liver, has enhanced necrosis, autophagy and apoptosis after IRI [8, 9], which is related to cirrhosis, liver failure and hepatocellular carcinoma progression [10]. Nonetheless, the underlying molecular mechanisms of the susceptibility of steatotic livers to IRI remain completely obscure.

Circular RNAs (circRNAs), a class of non-coding RNAs, are characterized by a covalent bond joining the 3' and 5' ends generated by back-splicing [11]. Different from linear RNAs, circular RNAs are more stable and not easily digested by RNase R due to the loss of cap and poly A tails [12]. Circular RNAs play essential roles in many biological processes, including transcription regulation, tumorigenesis and metabolic disorders. Massive researches have revealed that circRNAs may function as sponges for

microRNAs (miRNAs), interact with proteins to regulate gene expression, and translation into short-peptide [13]. Moreover, increasing evidences indicated the implication of circRNAs in liver diseases including hepatocellular carcinoma, non-alcoholic fatty liver (NAFLD), and hepatic IRI [14, 15]. However, data concerning their role in hepatic steatosis after IRI remain unexplored.

In this study, we comprehensively analyzed the features of differentially expressed circRNAs in high-fat diet(HFD) fed mice livers after hepatic IRI model. Through bioinformatics analysis, we found some signaling pathways of these circular RNAs and validated the alteration of their expression in our models. The expression of four down-regulated circRNAs in our models selected from RNase R digestion experiment was further investigated by qPCR. The circularity of screened circRNAs was also validated by gel electrophoresis and sanger sequencing. Therefore, this study suggested potential roles of circular RNAs in steatotic livers using a IRI mouse model, providing some efficient targets to alleviate the susceptibility of fatty livers to IRI.

## Materials And Methods

### Animals, diet, and hepatic IRI model

C57BL/6 wild-type (WT) mice were purchased from Shanghai SLAC Co. Ltd (Shanghai, China). Animal protocols were approved by the Institutional Animal Care and Use Committee of Renji hospital, School of Medicine, the Shanghai Jiao Tong University. 4- to 6-week-old male mice (14-16g) C57BL6 mice were fed a high-fat diet (HFD; 18.1% protein, 61.6% fat and 20.3% carbohydrates; D12492, Research Diets, New Brunswick, NJ) for 24 weeks to build a mouse model of liver steatosis. Mice were housed in a standard environment at 22 to 24°C with a 12:12 h light-dark cycle and ad libitum access to food and water. Successfully established HFD mice received liver IRI treatment as published [30]. In short, arterial and portal venous blood supply to the cephalad lobes of the liver were interrupted with an atraumatic clip for 90 min, and mice were sacrificed after reperfusion for 6h.

### Histology

Liver tissue sections were stained with hematoxylin-eosin (H&E) according to standard procedures. Oil red O (ORO) (O0625; Sigma-Aldrich, St Louis, MO) staining were performed following previously described protocol [31].

### Enzyme-linked immunosorbent assay (ELISA)

ELISA kits were used to detect mouse IL-6 and TNF- $\alpha$  (NeoBioscience Technology, Shenzhen, China) levels following the manufacturer's instructions.

### Biochemical analysis

Serum alanine aminotransferase (ALT) and aspartate aminotransferase (AST) levels were detected by microplate test kits (Nanjing Jianchen Bioengineering Institute, Nanjing, China) according to the

manufacturer's instructions [32].

## RNA-seq

Total RNA was extracted from separated liver tissue using the RNeasy Mini Kit (Qiagen, Hilden, Germany) following the manufacturer's instructions. Then nanoDrop 2000 (Thermo Fisher, Waltham, MA) were applied for the quality and concentration of the isolated RNA. Before circRNA sequencing, we used RNase R (Geneseed, Guangzhou, China) to remove the linear RNAs from total RNA. We contrasted cDNA library with one microgram of the RNA by VAHTSTM mRNA-seq v2 library Prep Kit for illumina (Vazyme, Nanjing, China). Next, the fragmented RNA and double-stranded cDNA was synthesized. In addition, we performed ligation of cDNA fragments to the adapter for end repair and A-addition as reported before. Then the ligated cDNA was amplified by PCR. Illumina Hiseq 2500 was employed for RNA-sequencing [33]. Quantile normalization and further data analysis were conducted by R software. The differentially expressed circular RNAs were selected according to a standard of fold-change and p value (p-value < 0.05 and fold change > 2.0).

## Validation of circRNAs

We designed divergent and convergent primers to subsequent analyze these circRNAs. The details of primers were exhibited in Supplementary Table 1. PCR products of divergent primers were then collected and sequenced to examine the back-splicing sites of circRNAs. We performed RNase R (Geneseed, Guangzhou, China) digestion experiment to detect the stability of circRNAs according to the manufacturer's instructions. In short, 2 µg RNA was digested in 8 U RNase R for 10 min at 37°C and then repurified it through the RNeasy Mini Kit.

## cDNA synthesis and quantitative real-time PCR (Q-PCR)

A total of 1 µg RNA was prepared for reverse transcription with PrimeScript RTreagent Kit (Takara, Tokyo, Japan). QPCR was conducted using a SYBR Green PCR Kit (Takara) following the manufacturer's instructions. The β-actin was used as reference gene for circRNAs. The qPCR was programmed with the CFX 96 q-PCR system (BIO-RAD, Hercules, CA, USA) as follows: 95°C for 5 min; 40 cycles of 95°C for 10 s, 60°C for 34 s. The relative expression of circRNAs was evaluated by  $2^{-\Delta\Delta Ct}$  method. The primer sequences information was displayed in Supplementary Table 1.

## GO analysis and KEGG pathway analysis of host genes

GO analysis (<http://www.geneontology.org>) was applied to understand the corresponding host genes of differentially expressed circRNAs. Likewise, following the annotation of the KEGG (<http://www.kegg.jp/kegg>) [34,35], we disclosed the significant pathways connected with differentially expressed circRNAs.

## Statistical Analysis

Results are expressed as the mean  $\pm$  SEM. The results were analyzed using two-tailed, unpaired or paired Student's *t*-test.  $p < 0.05$  was considered statistically significant (\*= $p < 0.05$ /\*\*= $p < 0.01$ /\*\*\*= $p < 0.001$ ).

## Results

### HFD-fed mice developed steatosis and aggravated hepatic IRI

HFD mice developed steatotic livers imitating human obesity [16]. As shown in Oil Red-O (ORO) staining (Fig. 1a), 24-week HFD-fed mice were characterized by liver steatosis. To further validate the successful establishment of liver steatotic models, we next performed hepatic IRI models. By detecting the alanine transaminase (ALT) and aspartate transaminase (AST) levels in serum, which were significantly elevated in mice after IRI compared with sham controls both in normal control diet (NCD) and HFD groups (Fig. 1b-c). Consistent with prior research conclusions [17], hepatic damage extent, illustrated by AST and ALT levels, was significantly enhanced in animals with steatotic livers compared with NCD mice after IRI (Fig. 1b-c). We also determined the cytokines levels. As shown in Fig. 1d-e, TNF- $\alpha$  and IL-6 concentrations were strikingly increased in IRI mice compared to sham group both in NCD and HFD models, which disclosed the inflammation was exacerbated in IRI mice following NCD or HFD. Furthermore, we employed HE staining to examine hepatic histological changes in HFD-diet mice with IRI. Results displayed there were severe necrosis area in steatotic liver after IRI model. The necrosis area was contoured by dashed line (Fig. 1f). In general, all above results indicated that the mouse models of liver steatosis and liver IRI based on steatosis were successfully established.

### Bioinformatics analysis of circular RNAs in steatotic livers after IRI model

RNA sequencing indicated the differential circular RNAs expression levels between IRI group and sham group in HFD mice (Fig. 2a). Then we performed a cluster heat-map analysis to further clarify the expression of these circRNAs (Fig. 2b). Next, by GO analysis, a total of 13 host genes were enriched in 223 GO terms. There were 6, 7, and 8 terms significantly changed in biological processes, cellular components and molecular functions, respectively (Fig. 2c). KEGG enrichment analysis was then performed for the parental genes of these circRNAs expressed differentially. A total of 26 pathways were enriched and the top 20 pathways were exhibited (Fig. 2d), including fat digestion and absorption, antigen processing and presentation, cell adhesion molecules (CAMs) and so on, which suggested these pathways might also be involved in the regulation of liver steatosis to IRI.

### Verification of the circularity of these differentially expressed circular RNAs in steatotic livers after IRI models

In order to verify the accuracy of RNA-sequencing, we randomly selected five differentially expressed circRNAs whose length ranged from 200 bp to 700 bp, including one up-regulated circular RNAs named chr3:83031528|83031748 as well as four down-regulated circular RNAs named chr10:89473752|89483524, chr16:18894774|18899457, chr4:72157463|72170770 and chr5:90531492|90545519 (table.1). The convergent and divergent primers were designed to detect the

back-splicing sequences of these circular RNAs. Above-mentioned circRNAs, as well as their host genes, were treated by RNase R to examine the stability of circRNAs.

Table 1  
RNA sequencing indicated five most obvious differentially expressed circular RNAs.

CircRNA_ID	Parental gene	Up/down	P-value
Chr3:83031528 83031748	Fga	Up	0.002
Chr10:89473752 89483524	Nr1h4	Down	0.018
Chr16:18894774 18899457	Hira	Down	0.044
Chr4:72157463 72170770	Tle1	Down	0.007
Chr5:90531492 90545519	Afm	Down	0.008

QPCR results displayed that except the up-regulated circRNA chr3:83031528|83031748 (Fig. 3e), the expression of other four circular RNAs had no significant differences between RNase R treatment and mock group, while their parental genes were strikingly decreased (Fig. 3a-d).

Next, these four down-regulated circRNAs were further picked out to verify the accuracy of RNA-sequencing. As shown in agarose gel electrophoresis (Fig. 4), the products could be amplified by convergent primers with either cDNA or gDNA added as template, while divergent primers could only amplify products by using cDNA as template.  $\beta$ -actin was used as negative control. Sequence alignment of their junction positions provided identical sequences by sanger sequencing following gel electrophoresis, all these results demonstrating the circularity of these circular RNAs expressed differentially (Fig. 5).

Validation of differentially expressed circular RNAs in steatotic livers after IRI models by qPCR

To investigate the expression of circular RNAs and further confirm they might play critical roles in regulating IRI after liver steatosis, we employed qPCR to determine the differential expression of certain circular RNAs mentioned above. According to qPCR data, the expression of circRNAs validated by RNA-sequencing and qPCR are highly consistent (Fig. 6a). Chr10:89473752|89483524, chr16:18894774|18899457, chr4:72157463|72170770 and chr5:90531492|90545519 were drastically decreased in IRI tissues with liver steatosis compared with HFD-fed sham mice. To better prove these differentially expression of circRNAs between IRI group and sham group were particularly in steatotic IRI livers, we established simple IRI models with normal chow diet (NCD) fed. QPCR results showed that the expression of chr10:89473752|89483524, chr16:18894774|18899457 and chr5:90531492|90545519 had no significant differences in NCD/IRI and NCD/SHAM models, while chr4:72157463|72170770 ( $P < 0.05$ ) was increased (Fig. 6b), suggesting that these circRNAs specifically decreased in HFD induced steatotic

IRI mice. In general, we screened some circular RNAs that expressed differentially in steatotic livers after IRI.

## Discussion

In this study, we established a mouse model of steatotic liver IRI. RNA sequencing was performed, and some differentially expressed circular RNAs were screened in steatotic liver during IRI compared with steatotic sham control. CircRNAs were further assayed by bioinformatics analysis. Briefly, this work revealed the potential role of circular RNAs in steatotic livers using a mouse model of IRI, providing novel clues to alleviate the susceptibility of fatty livers to ischemia/reperfusion injury.

Obesity is a global challenge in nowadays society [5]. With increasing incidence of NAFLD, a major complication of obesity, the higher risk of postoperative morbidity and mortality after transplantation surgery has been recognized [18]. Considerable scientific researches have been performed to illuminate this clinical phenomenon, and we have reached a consensus that hepatic steatosis is more sensitive to I/R injury [19, 20]. Conversely, the mechanisms whereby fatty liver sensitizes to IR damage remain largely unknown, and their elucidation might supply solutions to increase the graft load available for use in liver transplantation area. Studies have shown some possible mechanisms linked with this problem. For instance, in steatotic livers after IRI, MMP-9 may function as a promoter of PECAM-1 proteolytic breakdown and impact vascular integrity [21]. The blockade of CD8 and L-selectin attenuates hepatocellular injury in a fatty liver during IRI, confirming that CD8<sup>+</sup> cells are injury drivers in a steatotic liver [9]. Cholesterol and its trafficking to mitochondria critically contributes to the susceptibility of fatty liver to IRI [18]. All these findings involving metabolism, immunity, cellular dynamics may indicate the direction of future study.

The mechanism of the essential functions of circRNAs in organism is still not clear. During the past few years, a great number of circRNAs have been discovered in different tissues and diseases through high-throughput RNA sequencing, and a good few of them act as influential regulators in the occurrence and progression of diseases. For example, down-regulated circPVT1 levels in proliferating fibroblasts could trigger senescence. Moreover, circRNA levels were found to be significantly changed during cell proliferation in cancer progress [22]. CiSMARCA5, functions as a sponge for miR-17-3p/miR-181b-5p-TIMP3 in liver tissues and is significantly increased in hepatocellular carcinoma, indicating that the ciSMARCA5-miR-173p/miR-181b-5p-TIMP3 axis is upregulated in individuals with liver cancer [14].

Numerous researchers have proved that circular RNAs can compete with mRNAs for target binding sites of miRNAs to in turn regulate the expression of mRNAs [15, 23]. Furthermore, in recent years, the protein-binding function and the potentiality translating into short-peptide has attracted increasing attention [24, 25], which may give us some feasible clues in the future study. In fact, many non-coding RNAs have been identified and reported in ischemia/reperfusion injury [26]. In our study, we identified a total of 5480 circRNAs in liver IRI tissues following HFD-fed using RNA-sequencing analysis. In these circRNAs, 13 of them were differentially expressed between HFD/IRI and HFD/SHAM groups, and then we randomly

chose five circRNAs to verify the circularity of these circular RNAs by RNase R digestion experiment. Four stably expressed circRNAs were screened to validate the expression levels by qPCR. The results of qPCR and RNA-sequencing were largely identical, which indicated the reliability of RNA-sequencing.

We obtained 223 terms from GO enrichment analysis, including 127 biological processes, 65 molecular functions, and 31 cellular components. Antigen processing and presentation of exogenous peptide antigen via MHC class I, bile acid binding, response to peptide hormone, response to cytokine, protease binding, and glycoprotein binding were significantly enriched, these pathways might participate in the regulation of steatotic IRI. We suppose that several common signaling pathways may be regulated by circular RNAs to influence the liver IRI with steatosis. Up to now, several important pathways regulated by circRNAs have been reported in cancer progression, such as Wnt signaling pathway [27], MAPK signaling pathway [28], p-CDK2 pathway and NF-kappa B signaling pathway [29]. However, it is still unexplored how circular RNAs regulate steatotic IRI, and it is plausible that some specific signaling pathways dominate this process, which needs further investigation.

In conclusion, through RNA sequencing and Bioinformatics analysis, we found some differentially expressed circular RNAs in a liver steatotic IRI model. The circularity and possible signaling pathways of these circular RNAs have been demonstrated. Therefore, these circular RNAs may function as new therapeutic targets to attenuate the susceptibility of steatotic livers to IRI. Further studies are expected to explore the underlying mechanism of these circular RNAs in steatotic IRI pathological process.

## Abbreviations

IRI: Ischemia and reperfusion injury; CircRNA: Circular RNA; HFD: High-fat diet; NCD: normal chow diet; NAFLD: Non-alcoholic fatty liver; GO: Gene Ontology; KEGG: Kyoto Encyclopedia of Genes and Genomes; qPCR: Quantitative polymerase chain reaction

## Declarations

### Author Contributions

Conceptualization, Xiaoye Qu and Chao Zheng; Data curation, Xiaoye Qu and Xuehua Sun; Formal analysis, Xiaoye Qu and Bingrui Wang; Funding acquisition, Chao Zheng, Yueqiu Gao, Qiang Xia and Xiaoni Kong; Investigation, Xiaoye Qu and Fang Wang; Methodology, Xiaoye Qu and Chao Zheng; Project administration, Qiang Xia and Xiaoni Kong; Resources, Xiaoye Qu and Qiang Xia; Supervision, Qiang Xia and Xiaoni Kong; Validation, Xiaoye Qu and Chao Zheng; Writing – original draft, Xiaoye Qu; Writing – review & editing, Xiaoye Qu and Xiaoni Kong.

### Acknowledgements

We thank oebiotech co., Ltd. for the provision of the RNA-seq techniques.

## Competing interests

The authors declare no conflict of interest.

## Availability of data and materials

The datasets generated and/or analysed during the current study are available in the National Center for Biotechnology Information (NCBI) Sequence Read Archive (SRA) (accession number: PRJNA609716).

## Consent for publication

Not applicable.

## Ethics approval and consent to participate

This study was approved by the Institutional Animal Care and Use Committee of Renji hospital, School of Medicine, the Shanghai Jiao Tong University.

## Funding

This work was supported by the National Natural Science Foundation of China (81873582 and 81670562 to X Kong, 81904164 to C Zhen, 81874436 to Y Gao, 81670598 to Q Xia).

## References

1. Selzner M, Rüdiger HA, Sindram D, Madden J, Clavien P-A. Mechanisms of ischemic injury are different in the steatotic and normal rat liver: Mechanisms of ischemic injury are different in the steatotic and normal rat liver. *Hepatology*. 2000;32:1280–8.
2. Cameron AM, Ghobrial RM, Yersiz H, Farmer DG, Lipshutz GS, Gordon SA, et al. Optimal Utilization of Donor Grafts With Extended Criteria: A Single-Center Experience in Over 1000 Liver Transplants. *Annals of Surgery*. 2006;243:748–55.
3. de Rougemont O, Dutkowski P, Clavien P-A. Biological modulation of liver ischemia–reperfusion injury: Current Opinion in Organ Transplantation. 2010;15:183–9.
4. Gehrau RC, Mas VR, Dumur CI, Ladie DE, Suh JL, Luebbert S, et al. Regulation of Molecular Pathways in Ischemia-Reperfusion Injury After Liver Transplantation: *Transplantation Journal*. 2013;96:926–34.
5. Kopelman PG. Obesity as a medical problem. *Nature*. 2000;404:635–43.
6. Serafín A, Roselló-Catafau J, Prats N, Xaus C, Gelpí E, Peralta C. Ischemic Preconditioning Increases the Tolerance of Fatty Liver to Hepatic Ischemia-Reperfusion Injury in the Rat. *The American Journal of Pathology*. 2002;161:587–601.
7. Gupta NA, Kolachala VL, Jiang R, Abramowsky C, Romero R, Fifadara N, et al. The Glucagon-Like Peptide-1 Receptor Agonist Exendin 4 Has a Protective Role in Ischemic Injury of Lean and Steatotic

- Liver by Inhibiting Cell Death and Stimulating Lipolysis. *The American Journal of Pathology*. 2012;181:1693–701.
8. Hamada T, Fondevila C, Busuttil RW, Coito AJ. Metalloproteinase-9 deficiency protects against hepatic ischemia/reperfusion injury. *Hepatology*. 2007;47:186–98.
  9. Kolachala VL, Palle S, Shen M, Feng A, Shayakhmetov D, Gupta NA. Loss of L-selectin-guided CD8<sup>+</sup>, but not CD4<sup>+</sup>, cells protects against ischemia reperfusion injury in a steatotic liver: Liver Injury/Regeneration. *Hepatology*. 2017;66:1258–74.
  10. Jaeschke H, Woolbright BL. Current strategies to minimize hepatic ischemia–reperfusion injury by targeting reactive oxygen species. *Transplantation Reviews*. 2012;26:103–14.
  11. Chen L-L. The biogenesis and emerging roles of circular RNAs. *Nat Rev Mol Cell Biol*. 2016;17:205–11.
  12. Li X, Yang L, Chen L-L. The Biogenesis, Functions, and Challenges of Circular RNAs. *Molecular Cell*. 2018;71:428–42.
  13. Memczak S, Jens M, Elefsinioti A, Torti F, Krueger J, Rybak A, et al. Circular RNAs are a large class of animal RNAs with regulatory potency. *Nature*. 2013;495:333–8.
  14. Yu J, Xu Q, Wang Z, Yang Y, Zhang L, Ma J, et al. Circular RNA cSMARCA5 inhibits growth and metastasis in hepatocellular carcinoma. *Journal of Hepatology*. 2018;68:1214–27.
  15. Rong D, Lu C, Zhang B, Fu K, Zhao S, Tang W, et al. CircPSMC3 suppresses the proliferation and metastasis of gastric cancer by acting as a competitive endogenous RNA through sponging miR-296-5p. *Mol Cancer*. 2019;18:25.
  16. Li Z, Soloski MJ, Diehl AM. Dietary factors alter hepatic innate immune system in mice with nonalcoholic fatty liver disease. *Hepatology*. 2005;42:880–5.
  17. Jiménez-Castro MB, Casillas-Ramírez A, Mendes-Braz M, Massip-Salcedo M, Gracia-Sancho J, Elias-Miró M, et al. Adiponectin and resistin protect steatotic livers undergoing transplantation. *Journal of Hepatology*. 2013;59:1208–14.
  18. Llacuna L, Fernández A, Montfort CV, Matías N, Martínez L, Caballero F, et al. Targeting cholesterol at different levels in the mevalonate pathway protects fatty liver against ischemia–reperfusion injury. *Journal of Hepatology*. 2011;54:1002–10.
  19. Teoh NC. Hepatic ischemia reperfusion injury: Contemporary perspectives on pathogenic mechanisms and basis for hepatoprotection—the good, bad and deadly: Pathogenesis of hepatic ischemia reperfusion injury. *Journal of Gastroenterology and Hepatology*. 2011;26:180–7.
  20. Zaouali MA, Reiter RJ, Padriša-Altés S, Boncompagni E, García JJ, Ben Abennebi H, et al. Melatonin protects steatotic and nonsteatotic liver grafts against cold ischemia and reperfusion injury: Melatonin in steatotic liver preservation. *Journal of Pineal Research*. 2010;213-221.
  21. Kato H, Kuriyama N, Duarte S, Clavien P-A, Busuttil RW, Coito AJ. MMP-9 deficiency shelters endothelial PECAM-1 expression and enhances regeneration of steatotic livers after ischemia and reperfusion injury. *Journal of Hepatology*. 2014;60:1032–9.

22. Szabo L, Salzman J. Detecting circular RNAs: bioinformatic and experimental challenges. *Nature Reviews Genetics*. 2016;17:679–92.
23. Lu C, Chen B, Chen C, Li H, Wang D, Tan Y, et al. CircNr1h4 regulates the pathological process of renal injury in salt-sensitive hypertensive mice by targeting miR-155-5p. *J Cell Mol Med*. 2020;24:1700–12.
24. Li Q, Wang Y, Wu S, Zhou Z, Ding X, Shi R, et al. CircACC1 Regulates Assembly and Activation of AMPK Complex under Metabolic Stress. *Cell Metabolism*. 2019;30:157-173.e7.
25. Zhu P, Zhu X, Wu J, He L, Lu T, Wang Y, et al. IL-13 secreted by ILC2s promotes the self-renewal of intestinal stem cells through circular RNA circPan3. *Nat Immunol*. 2019;20:183–94.
26. Ye Z, Kong Q, Han J, Deng J, Wu M, Deng H. Circular RNAs are differentially expressed in liver ischemia/reperfusion injury model. *J Cell Biochem*. 2018;119:7397–405.
27. Ma Z, Shuai Y, Gao X, Wen X, Ji J. Circular RNAs in the tumour microenvironment. *Mol Cancer*. 2020;19:8.
28. Li Y, Zheng Q, Bao C, Li S, Guo W, Zhao J, et al. Circular RNA is enriched and stable in exosomes: a promising biomarker for cancer diagnosis. *Cell Res*. 2015;25:981–4.
29. Du WW, Yang W, Liu E, Yang Z, Dhaliwal P, Yang BB. Foxo3 circular RNA retards cell cycle progression via forming ternary complexes with p21 and CDK2. *Nucleic Acids Res*. 2016;44:2846–58.
30. Xu D, Chen L, Chen X, Wen Y, Yu C, Yao J, et al. The triterpenoid CDDO-imidazolide ameliorates mouse liver ischemia-reperfusion injury through activating the Nrf2/HO-1 pathway enhanced autophagy. *Cell Death Dis*. 2017;8:e2983–e2983.
31. Xu M, Wu H, Li M, Wen Y, Yu C, Xia L, et al. DJ-1 Deficiency Protects Hepatic Steatosis by Enhancing Fatty Acid Oxidation in Mice. *Int J Biol Sci*. 2018;14:1892–900.
32. Mitchell C, Willenbring H. A reproducible and well-tolerated method for 2/3 partial hepatectomy in mice. *Nat Protoc*. 2008;3:1167–70.
33. Lv C, Sun L, Guo Z, Li H, Kong D, Xu B, et al. Circular RNA regulatory network reveals cell–cell crosstalk in acute myeloid leukemia extramedullary infiltration. *J Transl Med*. 2018;16:361.
34. Yang B, Xia Z, Zhong B, Xiong X, Sheng C, Wang Y, et al. Distinct Hippocampal Expression Profiles of Long Non-coding RNAs in an Alzheimer’s Disease Model. *Mol Neurobiol*. 2017;54:4833–46.
35. Zheng Y, Hui T, Yue C, Sun J, Guo D, Guo S, et al. Comprehensive analysis of circRNAs from cashmere goat skin by next generation RNA sequencing (RNA-seq). *Sci Rep*. 2020;10:516.

## Figures

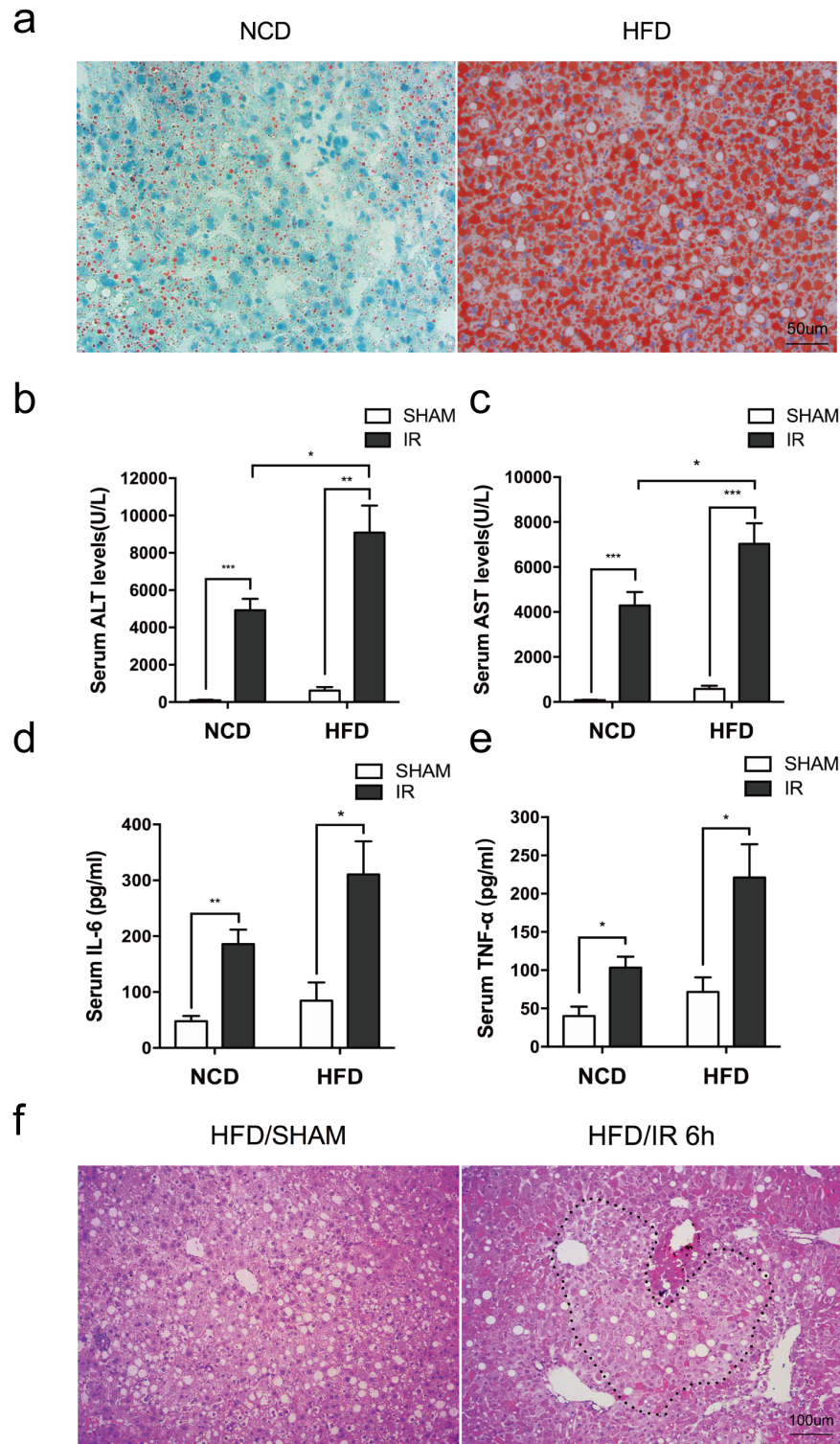


**Figure 1**

HFD-fed mice developed steatosis and aggravated hepatic IRI. Oil Red-O staining of 24-week HFD-fed mice and NCD control (a). The serum ALT (b) and AST (c) levels were significantly increased in HFD IRI mice compared with NCD IRI mice. d and e. Serum levels of TNF- $\alpha$  and IL-6 were significantly increased in steatotic livers after IRI. Representative necrotic area was shown in IRI models with steatosis (f). The statistical difference was determined by unpaired student's t-test.

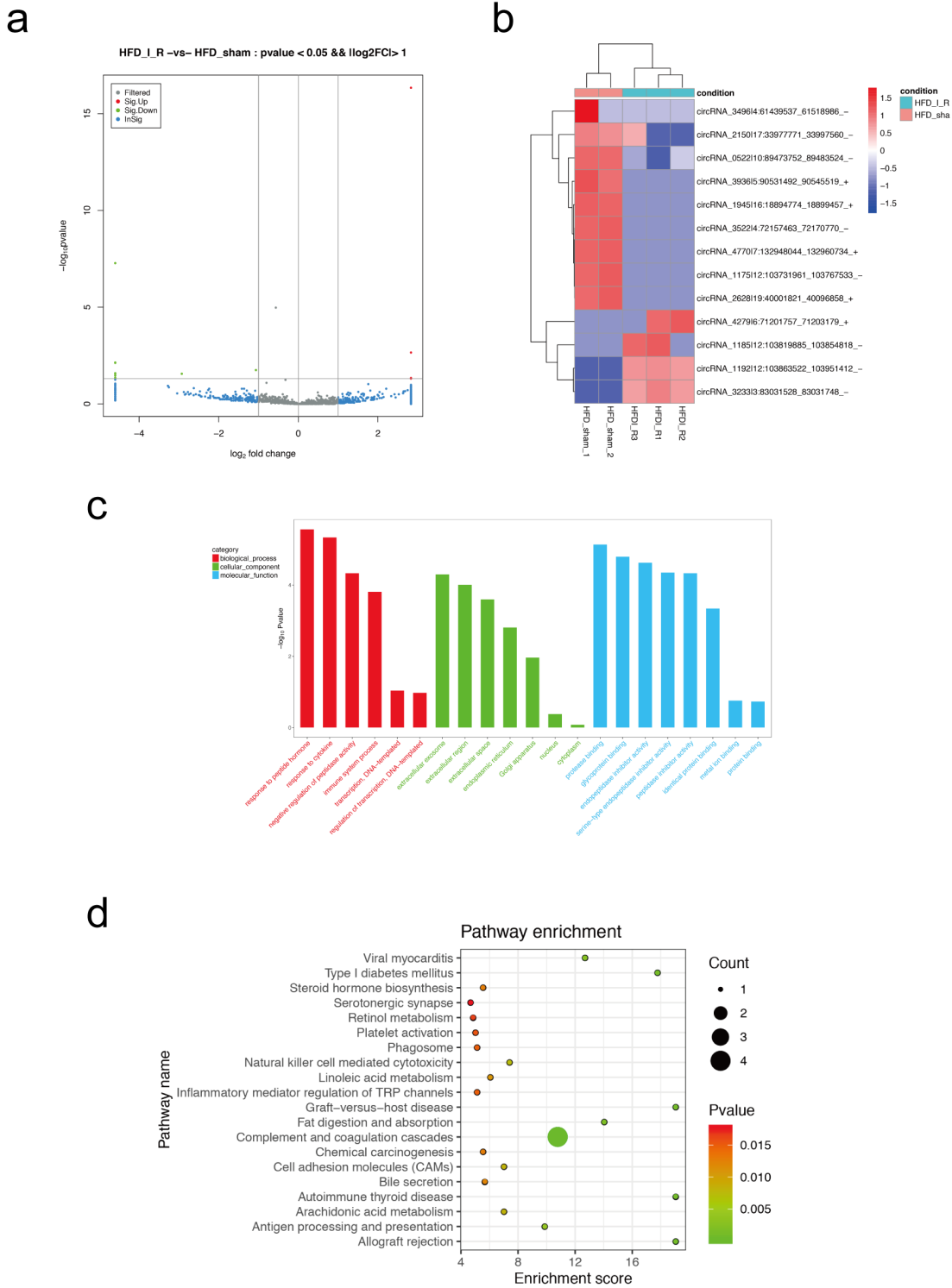


**Figure 2**

Analysis of circular RNAs expressed differentially in steatotic livers after ischemia and reperfusion injury model. a and b, Circular RNAs differentially expressed between HFD/IRI group and HFD/SHAM group. c, function of differentially expressed circular RNAs were indicated by GO analysis. d, KEGG analysis predicted functions and their key signaling pathways linked with differentially expressed circular RNAs.

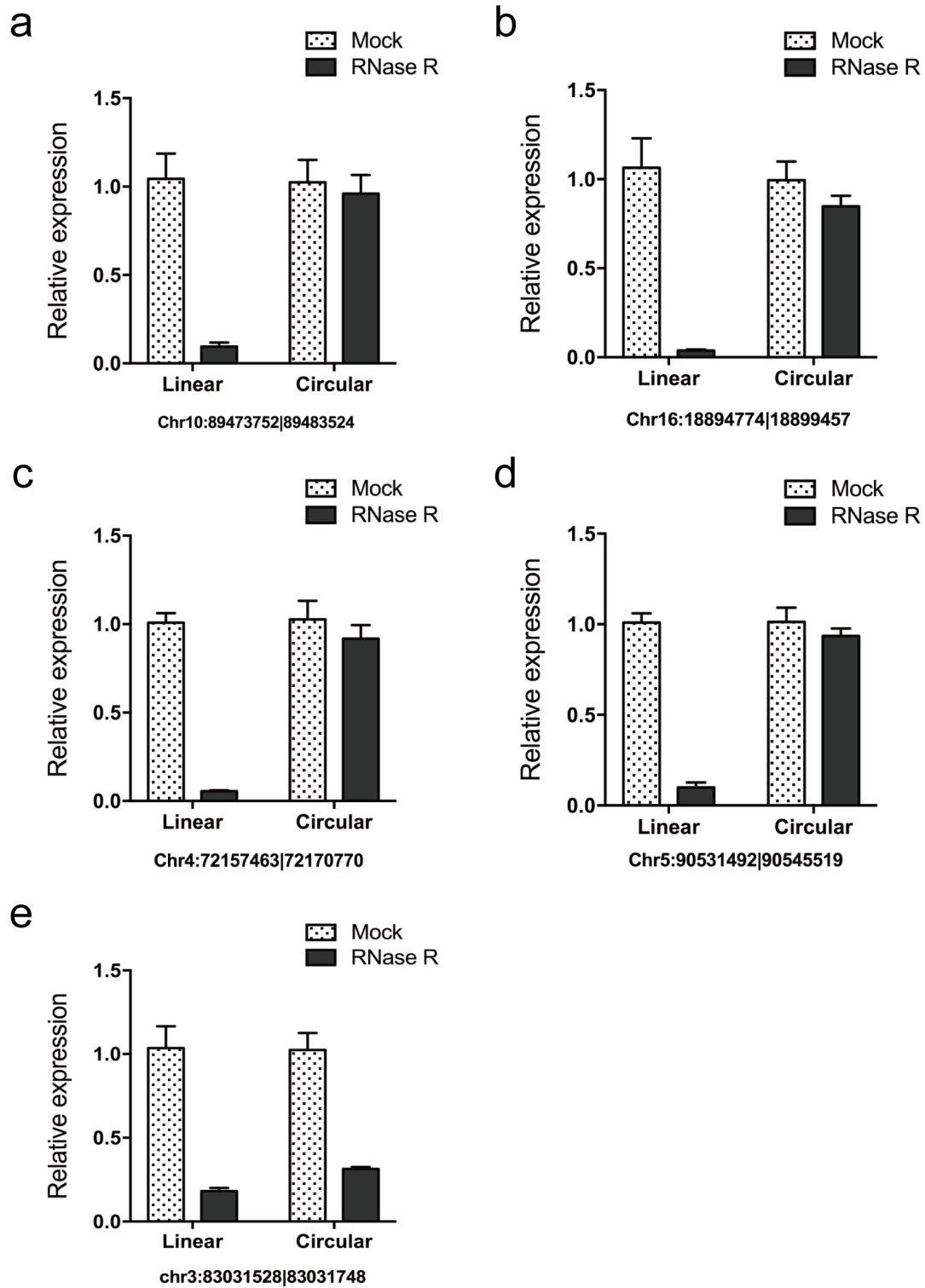


**Figure 3**

The circularity of circular RNAs in steatotic livers after ischemia and reperfusion injury model. a-d, four circular RNAs expression showed no significant differences between RNase R treatment and mock group, while one was significantly decreased after RNase R treatment (e).

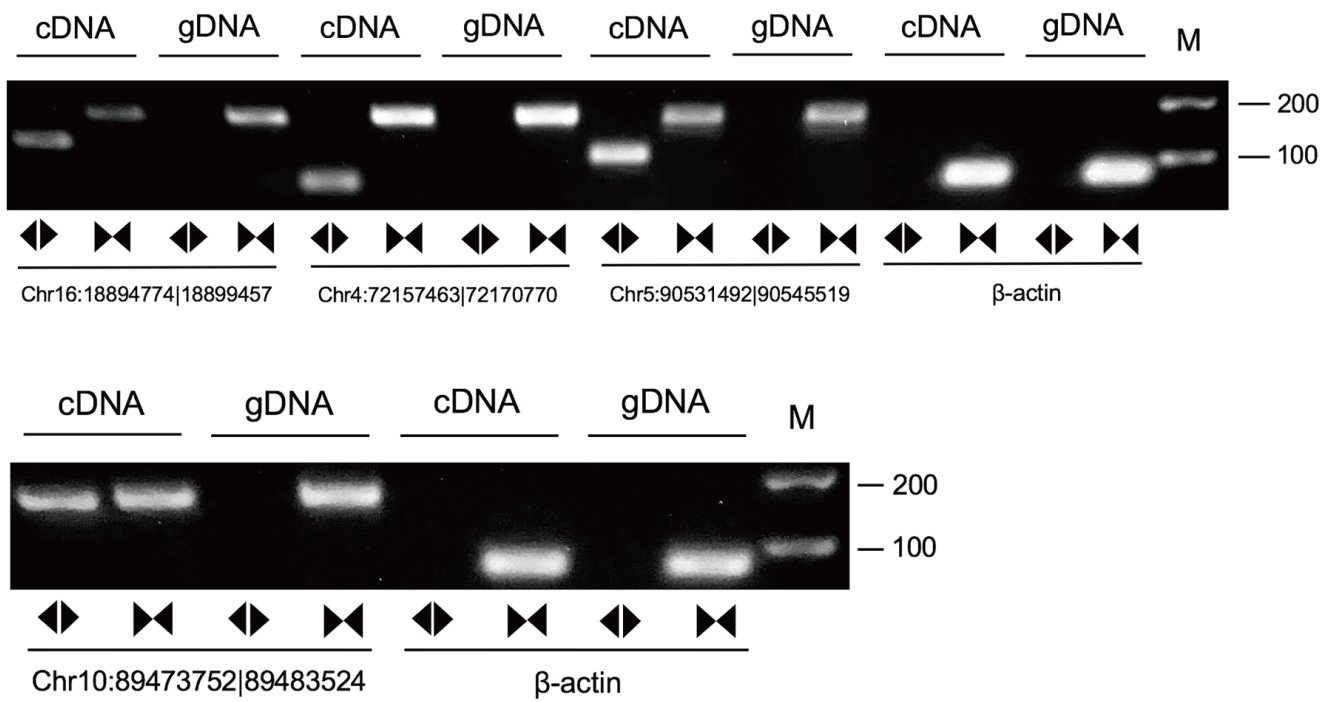


**Figure 4**

The circularity of circRNAs in steatotic livers after ischemia/reperfusion injury were determined by RT-PCR.

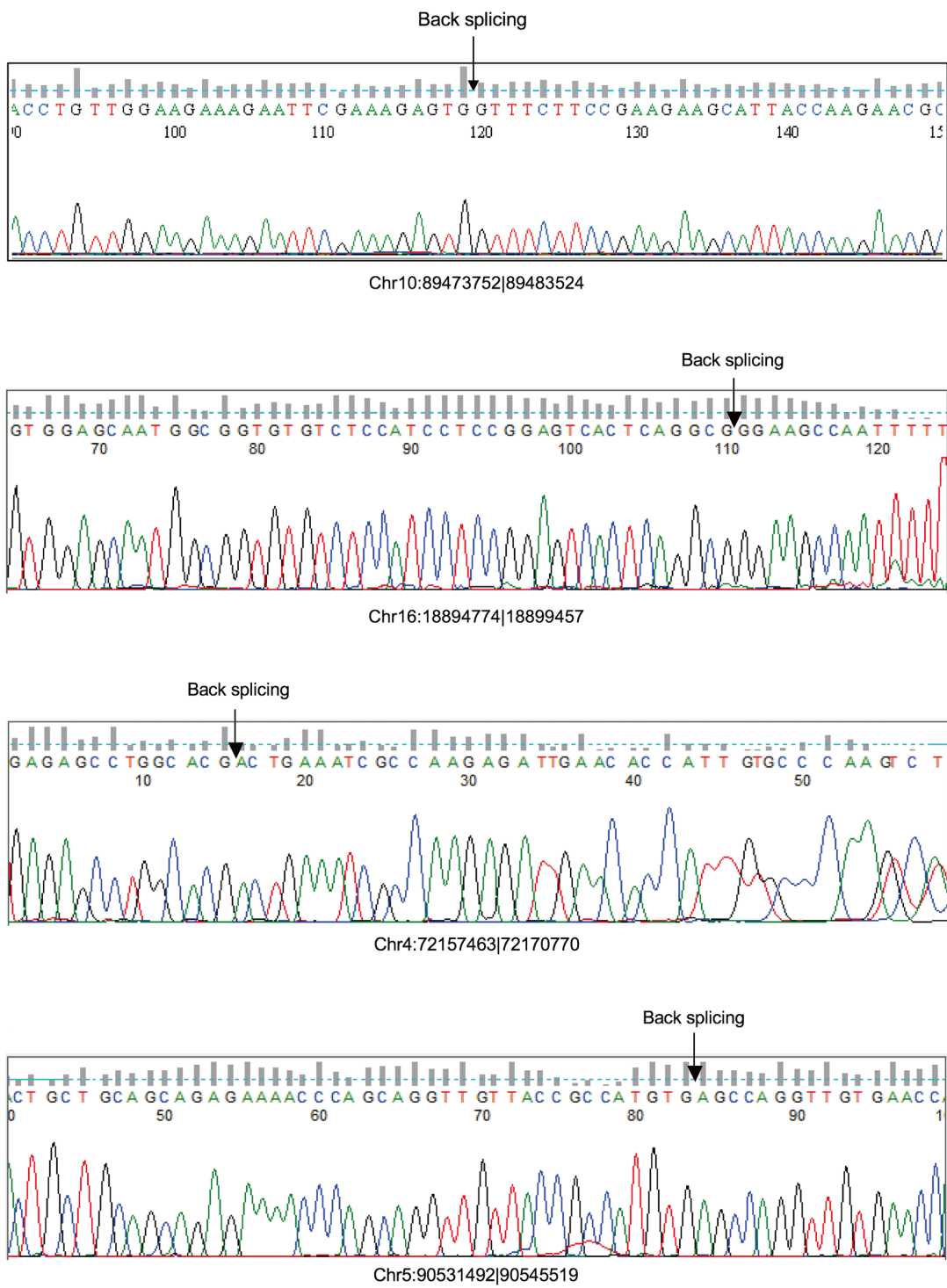


**Figure 5**

The circular sites of the circRNAs in steatotic livers after ischemia/reperfusion injury model. The back-splicing sites of four differentially expressed circular RNAs were analyzed through sanger sequencing.

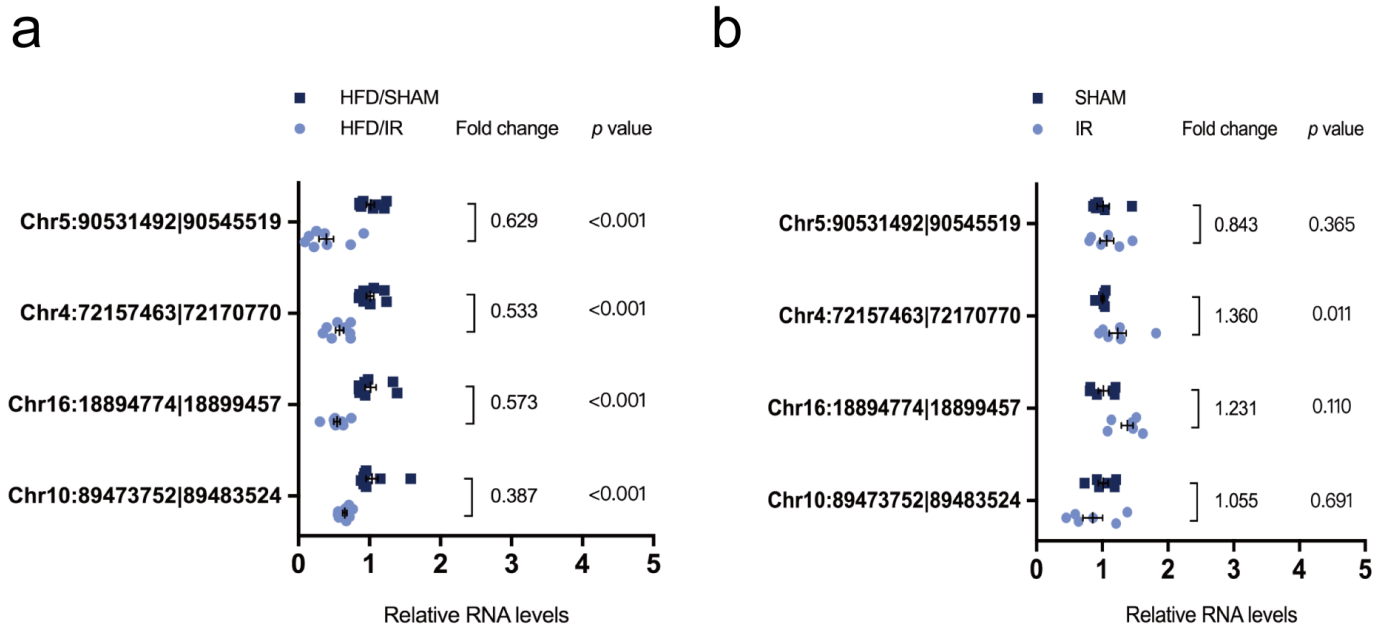


**Figure 6**

Verification of differentially expressed circRNAs in steatotic livers after ischemia and reperfusion injury by qPCR. a, Chr10:89473752|89483524, chr16:18894774|18899457, chr4:72157463|72170770 and chr5:90531492|90545519 were significantly decreased in IRI tissues with liver steatosis compared with HFD-fed sham mice (n= 8 mice/group). b, the expression of chr10:89473752|89483524, chr16:18894774|18899457 and chr5:90531492|90545519 had no significant differences in IRI models, and chr4:72157463|72170770 was increased in IRI mice comparing with sham controls (n= 6 mice/group).

## Supplementary Files

This is a list of supplementary files associated with this preprint. Click to download.

- [Additionalfile1.xls](#)